

The Three-Dimensional Arrangement of the Myocytes Aggregated Together Within the Mammalian Ventricular Myocardium

MORTEN SMERUP,^{1*} EVA NIELSEN,¹ PETER AGGER,¹ JESPER FRANDBSEN,²
PETER VESTERGAARD-POULSEN,² JOHNNIE ANDERSEN,³
JENS NYENGAARD,³ MICHAEL PEDERSEN,⁴ STEFFEN RINGGAARD,⁴
VIBEKE HJORTDAL,¹ PAUL P. LUNKENHEIMER,⁵ AND ROBERT H. ANDERSON⁶

¹Department of Cardiothoracic & Vascular Surgery, Aarhus University Hospital, Skejby, Denmark

²Center for Functionally Integrative Neuroscience, Aarhus University Hospital, Aarhus Sygehus, Denmark

³Stereology and EM Laboratory and MIND Center, Aarhus University, Denmark

⁴MR Research Center, Aarhus University Hospital, Aarhus, Denmark

⁵Klinik und Poliklinik für Thorax-, Herz- und Gefäßchirurgie, University Münster, Münster, Germany

⁶Cardiac Unit, Institute of Child Health, University College, London, UK

ABSTRACT

Although myocardial architecture has been investigated extensively, as yet no evidence exists for the anatomic segregation of discrete myocardial pathways. We performed post-mortem diffusion tensor imaging on 14 pig hearts. Pathway tracking was done from 22 standardized voxel groups from within the left ventricle, the left ventricular papillary muscles, and the right ventricular outflow tract. We generated pathways with comparable patterns in the different hearts when tracking from all chosen voxels. We were unable to demonstrate discrete circular or longitudinal pathways, nor to trace any solitary tract of myocardial cells extending throughout the ventricular mass. Instead, each pathway possessed endocardial, midwall, and epicardial components, merging one into another in consistent fashion. Endocardial tracks, when followed towards the basal or apical parts of the left ventricle, changed smoothly their helical and transmural angulations, becoming continuous with circular pathways in the midwall, these circular tracks further transforming into epicardial tracks, again by smooth change of the helical and transmural angles. Tracks originating from voxels in the papillary muscles behaved similarly to endocardial tracks. This is the first study to show myocardial pathways that run through the mammalian left and right ventricles in a highly reproducible manner according to varying local helical and transmural intrusion angles. The patterns generated are an inherent feature of the three-dimensional arrangement of the individual myocytes aggregated within the walls, differing according to the regional orientation and branching of individual myocytes. We found no evidence to support the existence of individual muscles or bands. *Anat Rec*, 292:1–11, 2009. © 2008 Wiley-Liss, Inc.

*Correspondence to: Morten Smerup, Department of Cardiothoracic & Vascular Surgery, and Clinical Institute, Aarhus University Hospital, Skejby, Brendstrupgaardsvej, 8200 Aarhus N, Denmark. Fax: +4589496016.
E-mail: morten.smerup@ki.au.dk

Received 25 March 2008; Accepted 27 August 2008

DOI 10.1002/ar.20798

Published online 2 December 2008 in Wiley InterScience (www.interscience.wiley.com).

Key words: myocardium; diffusion tensor magnetic resonance imaging; animal experimental models

Histological studies show that the myocardium making up the ventricular wall of mammals is composed of elongated contractile cells, the myocytes, which are embedded in a matrix of connective tissue (Lev and Simkins, 1956; Grant, 1965). According to traditional views, the myocytes are connected end-to-end in serial fashion, with the long axis of the aggregated cells orientated parallel to the tangential plane of the walls. It has long been shown, using anatomical dissections (Pettigrew, 1864), and confirmed histologically (Streeter et al., 1969), that the long axes of the tangentially oriented myocytes are also inclined at angles relative to the equatorial plane, with these so-called helical angles varying according to the depth of the myocytes aggregated within the ventricular walls. These studies showed that the myocytes in the subepicardial mural layers take a left-handed helix, with the cells within the midportion of the walls orientated in circular fashion, and those aggregated in the subendocardial layers tracing a right-handed helix, the helical angles themselves changing smoothly through the depths of the walls so that it is not possible to identify discrete layers separated one from the other by discrete arrangements of the supporting fibrous tissue matrix.

Despite multiple investigations in the last century that confirmed these traditional views, it has become fashionable within the past decade for researchers to postulate some degree of secondary and tertiary arrangement within the myocardial mesh. Examples of such purported organization are the concept of a unique myocardial band, proposed by Torrent-Guasp and his followers (Torrent-Guasp, 2005; Torrent-Guasp et al., 2001), the notion of “nested pretzels” put forward by Jouk and colleagues (Jouk et al., 2000), and the hypothesis that the myocytes are arranged in radial laminar sheets (LeGrice and associates, (LeGrice et al., 1995). None of these proposals, however, has been validated by anatomical or histological examinations that have explored the entirety of the left ventricular mass. Despite this lack of validation, the theories are now used by many researchers to explain the complex dynamics of myocardial rearrangement during the cardiac cycle (Costa et al., 1999; Harrington et al., 2005). It is crucial, therefore, that these new hypotheses should be investigated in objective fashion, the more so since other recent studies have shown that, in addition to their end-to-end connections, the myocytes are also linked in side-to-side fashion within a three-dimensional mesh (Dorri et al., 2007). Furthermore, despite the prevailing wisdom that all myocytes are orientated tangential relative to the ventricular walls, histological studies have now revealed the existence of populations of myocytes orientated with their long axis aligned transmurally to varying degree (Lunkenheimer et al., 2006). The technique of diffusion tensor magnetic resonance imaging (DTMRI) now provides the means to examine the orientation of the myocytes aggregated together within the entirety of the ventricular mass (Hsu et al, 1998). As has been shown previously, the mean orientation of the long axis of the

myocytes within small sample volumes is accurately reflected by the orientation of the largest value of diffusion, known as the primary eigenvector. We have used this technique, therefore, to explore several hypotheses. First, that the averaged long axis of myocytes confined within small volumes of the ventricular wall is not exclusively tangential, but rather intrudes or extrudes to a varying extent from the epicardium to the endocardium. Second, that the myocytes are aggregated within the fibrous matrix so as to produce a potentially infinite number of pathways throughout the myocardium, albeit that the number and vectors of the intercellular connections permit identification of a distribution of diversion for any chosen small myocardial volume. Third, in accordance with these hypotheses, it should be possible to trace reproducible patterns of connected myocytes within the ventricular walls, given that these tracks are not anatomically constrained by the organization of the fibrous matrix, and cannot be traced by gross dissection to reveal purported structures such as bands or pretzels. The concept of myocardial sheets composed of myocytes grouped in layers three to four cells thick cannot be proven or disproven by investigation of the primary eigenvector alone, since these structures are said to arrange themselves in planar or lamellar superstructures. The validity of the concept of sheets, therefore, will be the topic of a subsequent investigation.

MATERIALS AND METHODS

Animal Experiments

Our studies were made in hearts obtained from 14 Danish landrace female pigs, each pig weighing 20 kg. Prior to the experiments, the animals were kept at their usual farming facilities with unrestricted diet and water supply. Artificial daylight was maintained for 12 hr from 8 AM to 8 PM. Before being transported to the experimental laboratory, the animals received 10 mg midazolam intramuscularly to allow intravenous access; hereafter animals received 10 mg midazolam and 100 mg ketaminol intravenously to induce anaesthesia, and were intubated endotracheally and coupled to a ventilator (Siemens Servo 900D; Siemens-Eléma AB, Solna, Sweden). The ventilated minute volume was kept at 150 mL/kg, with a positive end-expiratory pressure of 4 cm water, and an FiO₂ of 50%. Muscular relaxation was achieved with 4 mg pancuronium given intravenously. Continuous anaesthesia consisted of 2–3% of isoflurane in the inhaled gases, while analgesia was provided by fentanyl intravenously (10 µg/kg/hr). The animals were placed in the supine position, and a median sternotomy was made to expose the heart. Heparin was administered intravenously (10,000 IU) to avoid post-mortem clotting. The animals were killed by excising the heart and great vessels. One liter of direct potassium rich cold cardioplegic solution (Kardioplex St. Thomas no. 1; H/S Apoteket, Copenhagen, Denmark) was administered selectively through the orifices of the coronary arteries at a pressure of ~100 mmHg at the

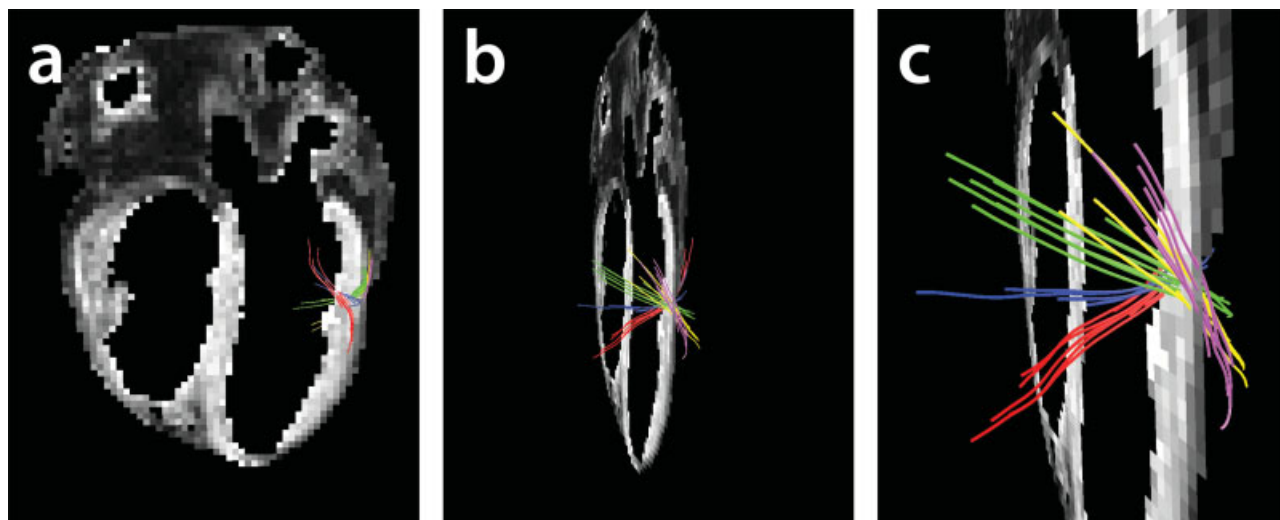


Fig. 1. The transmural distribution of the helical angle. Pathways of approximately two centimeters are shown across the left ventricular free wall in images (a–c). The red track represents the endocardial chains of myocytes and the magenta track represents the epicardial myocytes. These images were used to calculate the helical angles as outlined in the text.

point of the catheter tip. The heart was then immersed in the same cold cardioplegic solution for ~ 1 hr, following which a water-based MRI compatible polymer (Histomer) was injected through the atrioventricular valves so as to distend the ventricles to an end-diastolic state. This was possible since the hearts had been arrested in diastole, the injection caused the atrioventricular valves to close around the tip of the syringe, and any residual polymer was allowed to escape from the ventricles through the arterial valves. The heart was then immersed and allowed to float freely, in cardioplegic solution for another hour while the polymer hardened, thus avoiding any distortion of shape. Isotonic saline was next perfused through the coronary arteries to wash out the cardioplegic solution, and the myocardium was perfusion-fixed with formalin (Lillie's solution, 4 %, pH = 7.4) in the same manner, but with a pressure of ~ 100 mmHg at the point of the catheter tip. We perfused the saline first having made the empiric observation that it significantly lessened the myocardial contracture subsequent to perfusion with formaldehyde. The heart was suspended in formalin for 1–3 days, after which the formalin was substituted with phosphate buffered solution (PBS, pH = 7.4), and then stored at 4°C .

Diffusion Tensor Magnetic Resonance Imaging

The hearts were allowed to adjust to room temperature for 3 hr prior to scanning. MRI examinations were performed with a Philips Achieva 1.5 T clinical system (Philips Medical Systems, Best, Netherlands), equipped with Nova Dual Gradients and Software Release 2.1.3. The heart was placed in the magnet oriented with the long axis of the left ventricle aligned parallel to the axis of the main magnetic field. After scout imaging, a diffusion tensor MRI measurement was performed with a multi-slice (48 slices) 2D spin echo sequence using the following imaging parameters: slice thickness 1.3 mm, field-of-view $170 \times 101 \text{ mm}^2$, matrix 128×76 , giving an

isotropic resolution of 1.3 mm, repetition time 3900 msec, echo time 72 msec. We acquired 32 diffusion sensitive images with diffusion directions isotropic distributed with $b = 1271 \text{ sec}^{-1}$ and 1 image with $b = 0$. The total scan time was 16:20 hr. After imaging, the heart was immersed in PBS solution, and stored at 4°C prior to histologic examination.

Quantitative Analysis

Using custom-made software, we calculated the primary diffusion eigenvector of each voxel, normalizing the value at each voxel according to the values of the matrix as a whole to achieve comparability between different hearts. Quantitative analysis as outlined below was performed according to principles used by others so as to ensure the comparability of our data to that of other studies (Hsu et al., 1998; Holmes et al., 2000). In short, here the helical angle is defined as the projected angle of myocytes onto the tangential plane of the epicardium in any myocardial region measured relative to the equatorial plane of the left ventricle, the angles varying at different depths within the ventricular walls (Fig. 1). We assessed such helical angles at the anterior, lateral, and posterior free walls of the left ventricle, along with the septum, measuring the angles relative to the equatorial plane midway between the apex and the base of the ventricle, this plane being approximately at the level of the papillary muscles. Because of the fixed size of the voxels, and varying myocardial mural thicknesses, the number of sampling voxels varied through the wall between animals, and between mural segments. To be able to perform statistical analysis, we normalized measurements to the proportional mural thickness, setting the endocardium to 0% and epicardium to 100%, and using a polynomial fit to inter- and extrapolate values. Accordingly, we measured helical angles at 5 depths within the walls. The transmural intrusion of aggregated chains of myocytes was assessed indirectly by

means of identification of pathways that progressed transmurally from endocardium to epicardium or from epicardium to endocardium.

Tracking

Initially, for each of our chosen voxels, we calculated a 3×3 symmetrically positive tensor matrix using multivariate linear fitting with routines from Numerical Recipes (Press et al., 2007). After diagonalization, we calculated the corresponding eigenvectors and eigenvalues. The eigenvector corresponding to the largest eigenvalue is taken to be an indication of the orientation locally of the aggregated chains of myocytes. To track the connections of the aggregated chains of myocytes, we used the streamline FACT routine, (Parker et al., 2003) which was slightly modified in our in-house tracking software. For stopping, we used voxel anisotropy (FA) below 0.15, or an angle for the eigenvector between adjacent voxels of greater than 43° . The tracking step size was arbitrarily set to 0.5 mm. Thereafter, the investigator selected the required number of voxels of interest from the total three-dimensional matrix. On the basis of the characteristics of the primary eigenvectors of all voxels in the total matrix, the algorithm then calculated any possible “track,” or “pathway,” which passed through the chosen voxel of interest. The paths were color-coded clearly to visualize up to eight structurally different pathways. Since the total three-dimensional matrix consists of $128 \times 128 \times 128$, or 2,097,152 voxels, of which approximately 1/3 to 1/4 represents myocardium, we selected voxels at a few predetermined locations (Fig. 1), specifically the basal free wall of the left ventricle at subendocardial, midwall, and subepicardial depths, the midventricular free wall at the same depths, the apical wall, again at the same three depths, and the basal, midventricular, and apical parts of the septum, the latter points evaluating the right ventricular, midseptal, and left ventricular regions. We then chose groups of voxels in each of the paired papillary muscles of the mitral valve. In all, we selected 22 groups of voxels of interest. Since our software does not allow for simultaneous analysis of more than eight groups of tracks, and experience showed that information was obscured if more than six are chosen at a time, we interpreted the data using combinations of the tracks from the respective regions of interest. As a rule, we have shown the tracks as 3–6 increasing lengths of myocardial pathways since this facilitates the appreciation of the three-dimensional spatial orientation within the myocardium. As such the first of images in a sequence (with the shortest track progression) shows directly the origin of the pathways.

Statistical Analysis

Helical angles from regions of the myocardial walls were compared with MANOVA, using a level of significance of 5%. Myocardial pathways between hearts were compared by means of qualitative assessment of images so as to identify the characteristic appearances of the revealed tracks.

Ethical Considerations

All experiments were conducted after approval from the Danish Inspectorate of Animal Experimentation.

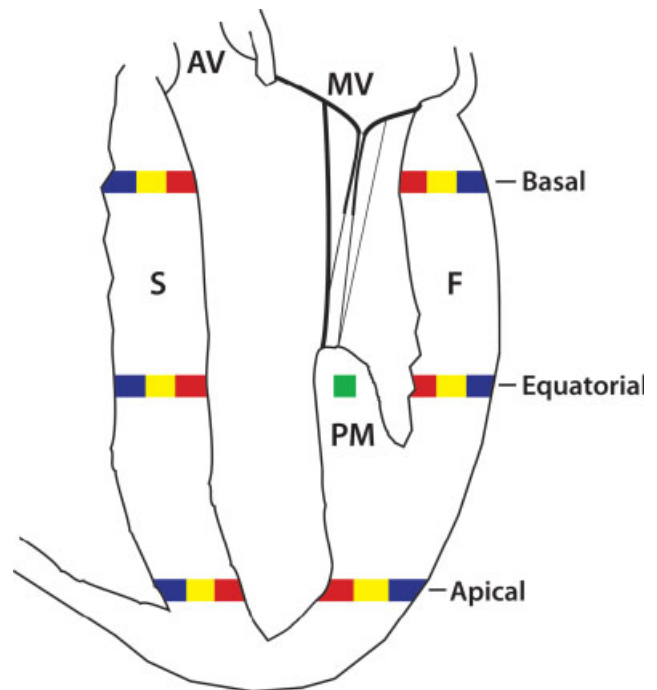


Fig. 2. A schematized image of the left ventricle showing the standardized placement of voxels throughout the septal and free walls of the myocardium at basal, equatorial and apical levels, respectively. The depth of the myocardium is shown by colors: red represents endocardium, yellow represents midwall myocardium, and blue represents epicardium or right ventricular septum. Green represents the papillary muscles of which only one is imaged. The voxels of the right ventricular outflow tract are not shown. AV: aortic valve; MV: mitral valve; PM: papillary muscle; S: septum; F: free wall.

Likewise the investigation conforms to the *Guide for the Care and Use of Laboratory Animals* published by the US National Institutes of Health (NIH Publication No. 85–23, revised 1996). The authors had full access to the data and take responsibility for its integrity. All authors have read and agree to the manuscript as written.

RESULTS

Quantitative Measurements

In Fig. 3, we show the helical angle as a function of transmural depth. The angles changed from $+65^\circ$ to $+20^\circ$ at the endocardium to -75° to -41° degrees at the epicardium, depending upon the region of the myocardial wall evaluated. Statistical analysis showed highly significant differences between regions (overall MANOVA $P < 0.001$).

Tracking

In all cases, it was possible to track virtual pathways from all chosen voxels of interest, with comparable patterns being generated from the different hearts (Figs. 4–8). Summarizing our findings, tracks commencing within the endocardial layers are oriented according to the pattern of a right hand helix, while epicardial tracks follow the pattern of a left hand helix. The tracks originating from the middle parts of the walls follow circular

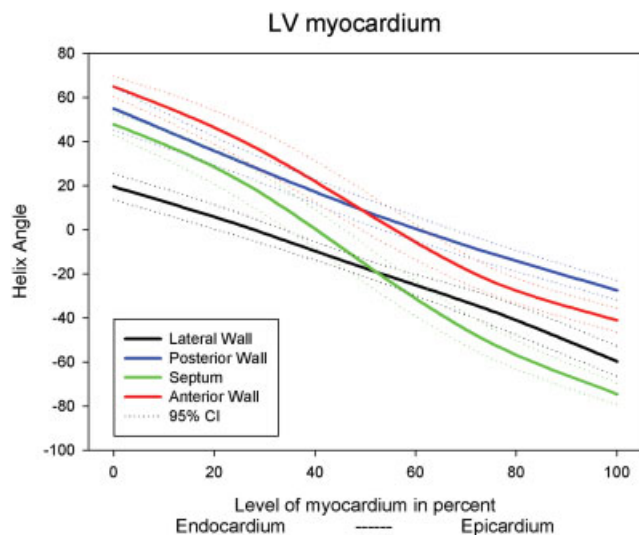


Fig. 3. The graph shows the transmurial distribution of the helical angle as function of myocardial depth in percent for the four wall segments: lateral, posterior, septal, and anterior. The endocardium is set to zero percent and the epicardium is set to 100%. The graph shows significant differences between the various wall segments of the left ventricle (MANOVA $P < 0.001$). Dotted lines represent 95 percent confidence intervals.

pathways around the cavity of the left ventricle. We could not distinguish discrete longitudinal or circular tracks, since the angles of inclination change smoothly when traced through the depth of the walls.

More interestingly, almost every generated track extends to encompass endocardial, midwall, and epicardial components (Figs. 4, 7, and 8), the parts merging in relatively consistent fashion. Thus, when endocardial tracks originating at any level, either from the parietal walls or the septum, are followed apically, they change both their helical and transmural angles smoothly, the endocardial tracks become continuous with circular components in the middle of the ventricular walls (Fig. 4). When traced further, these tracks continue smoothly to change both their helical and transmural angles, becoming continuous with epicardial or right ventricular septal tracks (Fig. 4). Such patterns are seen in reverse when following tracks originating endocardially toward the ventricular base. Such tracks again change their angulation in both equatorial and transmural planes, first becoming circular in the mid ventricular wall, and then extending to the epicardium. In similar fashion, epicardial pathways from at any location extend first into the middle of the wall, and thence to the endocardium, demonstrating a smooth and continuous transition of both helical and transmural angles (Fig. 4). Tracks originating from middle parts of the basal and equatorial walls of the left ventricle also follow this basic scheme, albeit that the changes in helical and transmural angulation are less pronounced, with massive aggregates following circular pathways that do not deviate much from their basal and equatorial positions (Fig. 5). Most of the ventricular apex is formed by tracks originating within the paired papillary muscles (Fig. 6). These tracks also follow the basic pattern described

above, commencing with a course comparable with the general endocardial trackings, but becoming exteriorized at the ventricular apex concomitant with tapering-off of the helical and transmural angles. Specific reciprocal trackings are seen at the apex, and at the base, of the left ventricle. At the base, the transition from endocardium through the midwall to the epicardium, or its reverse, occurs by spilling of right-handed helical aggregates over the rounded ventricular base, with spiraling round a circular axis placed in the transverse plane (Fig. 7). A similar transition is also found at the apex, albeit less distinct, with another right-handed helical transition occurring round a circular axis placed in the transverse plane (Fig. 6). Within most of the walls of the left ventricle, the continuous changes in helical and transmural angulation of the chains of interconnected myocytes produce three-dimensional figure-of-eight patterns (Figs. 4–8), which merge endocardially, within the middle parts of the walls, and epicardially. These pathways, nonetheless, represent predominant pathways within a continuum, rather than representing discrete morphological entities such as bands or toroids. We also found it possible to track pathways diverging in two principle planes from any given voxel of interest. These were the plane tangential to the epicardium, which showed greatest variation, and the transmural or transverse plane relative to the long-axis of the left ventricle, which had less variation (Figs. 4–8). Tracks entering the walls of the right ventricle, in their greater part, originated either from the septum or the parietal left ventricular walls. Tracking from voxels of interest placed specifically in the outflow tract of the right ventricle produced many pathways traversing or entering different parts of the left ventricle. In similar fashion, our seedings showed many different components for the left ventricle, including the papillary muscles. Our data could not be interpreted so as to provide evidence of any single ventricular myocardial band, nor for the existence of nested pretzels. Although we could not positively confirm the presence or absence of sheets, examination of our initial trackings produced no findings suggestive of radial organization of the aggregated myocytes. We are specifically examining the structure of the walls of the right ventricle in a companion investigation (work in progress).

DISCUSSION

To the best of our knowledge, ours is the first study of the intact heart showing a highly reproducible pattern of preferential pathways within the myocytes aggregated together to form the ventricular walls of the mammalian heart. The findings are entirely compatible with the illustrations produced by Pettigrew 150 years ago following careful dissection of the ventricular mass (Pettigrew, 1864). Wu and coworkers (2007) recently used similar DTMRI tracking to assess the distribution of oblique versus circular pathways within the ventricular walls, albeit not studying the entirety of the ventricular mass in structured fashion. Our trackings showed that, at any point within the three-dimensional myocardial mesh, the displayed pathways follow a predictable course, the pathways changing their direction smoothly and continuously in terms of the angulations of the long axis of the chains of myocytes relative to the epicardial surfaces

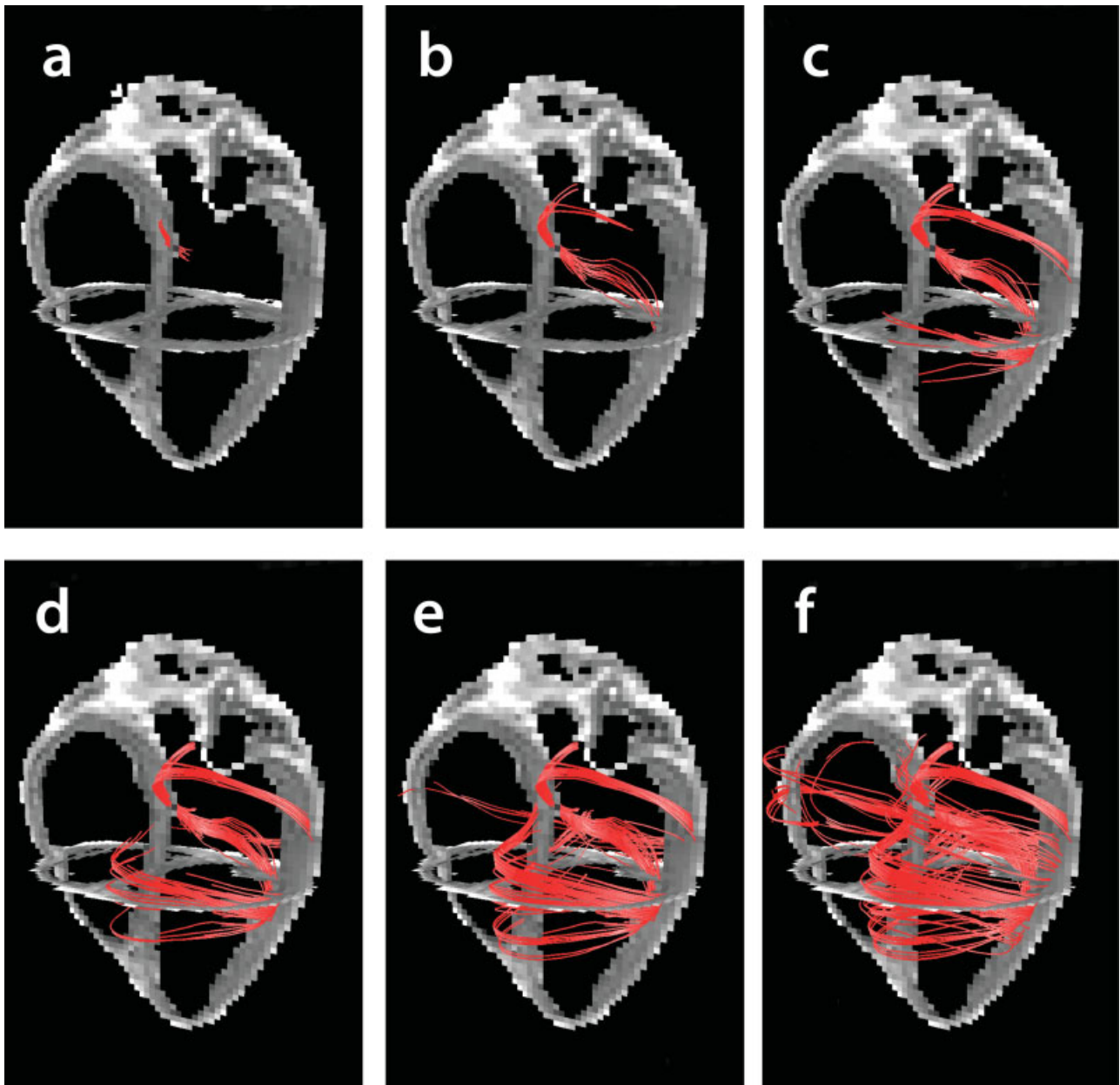


Fig. 4. Track progression from the basal septal endocardium. As tracks are evolving in images (a–f), the pathways are seen to change helical and transmural intrusion angles in a smooth and continuous manner so as to enable the tracks to connect distant endocardial, midwall, and epicardial regions. See text for further details.

and their depths within the walls. Pathways in the middle of the walls forming the basal and midventricular parts of the left ventricle display fewer changes in angulation, forming circular tracks that resemble closely the so-called “triebwerkzeug” as described by Krehl (Krehl, 1891). The patterning displayed, however, is not the consequence of discrete layering of connective tissue within the walls. Our findings, therefore, should not be interpreted as being indicative of the organization of the myocardium into discrete anatomical bundles, fibers, or tracts. Instead, our results support the notion that the

myocardium is arranged in the form of a three-dimensional mesh, the variations observed reflecting the orientation and branching of the individual myocytes in different regions of the walls.

Our findings are particularly pertinent, nonetheless, to ongoing discussions within the scientific community as to the existence of structures of higher order than the individual myocyte within the ventricular walls. Historical studies of cardiac anatomy are replete with numerous attempts to describe the myocardium in terms of isolated and easily recognizable tracts (Pettigrew, 1864;

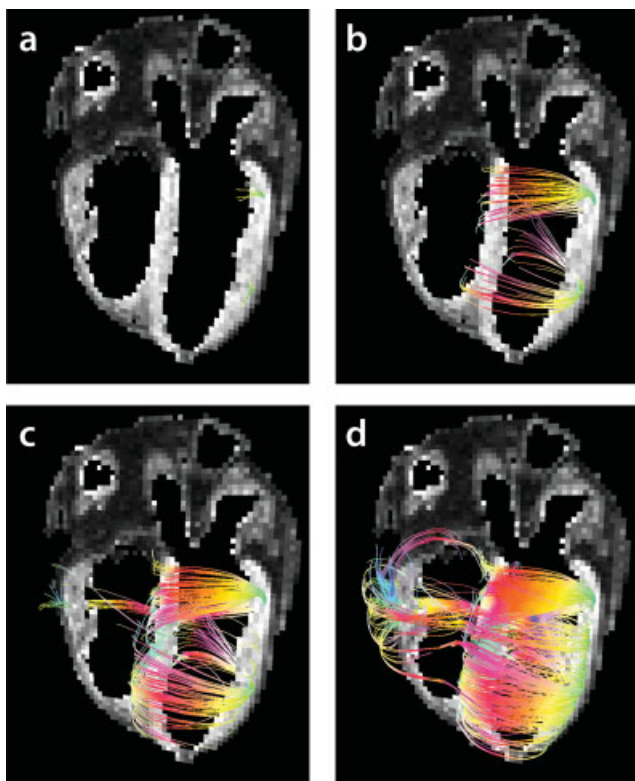


Fig. 5. Tracks from the midwall portion of the basal and equatorial left ventricular free wall. The tracks are color coded so that red, yellow, and green colors represent tracks that lie predominantly within a transverse plane of the left ventricle, while blue colors represent tracks that are parallel to the long-axis of the left ventricle. The figure shows that the midwall is occupied by circular tracks in correspondence with the so called Krehl's triebwerkzeug.

Mall, 1911; Torrent-Guasp, 2005; Jouk et al., 2000). Of these, two clearly defined concepts have attracted recent attention, namely the notion of a unique myocardial band, extending between the aorta and the pulmonary trunk (Torrent-Guasp, 2005; Torrent-Guasp et al., 2001), and the concept of nested pretzels (Jouk et al., 2000). Torrent-Guasp claimed that his band, revealed by dissection, also possessed a series of loops that encircled the cavities of both ventricles. This concept was then expanded to propose that wave-like excitation of the myocytes occurring along such a band could explain the complex interplay of ventricular contraction and relaxation in the cardiac cycle. The concept suffers from multiple flaws. First, it is impossible to reveal the band without disrupting the myocardial walls at multiple points. Second, the planes of cleavage purportedly permitting recognition of the parts of the band have never been demonstrated. Third, and perhaps most important, demonstration of the band is dependent exclusively on the skill and conviction of the dissector. The three-dimensional nature of the myocardium certainly allows dissection of a structure that resembles the purported band. It is not surprising, therefore, that partial elements of the artifact can be discerned from examination of our own findings. Validation of the concept, nonetheless, would require evidence that the myocytes are aggregated

exclusively from the pulmonary trunk to the aorta. Our results show unequivocally that this is not the case, and hence serve to disprove the notion of the unique myocardial band.

In very recent studies, others have used polarized light microscopy to assess the pattern of the myocytes as aggregated within the fetal human heart (Jouk et al., 2000). Extending the previous theories of Streeter and associates, these authors have concluded that chains of myocytes run in geodesic fashion on toroidal surfaces in the myocardium. The account given for the three-dimensional structure of the myocardium by these proponents, however, is just as misplaced as the inappropriate concept of a unique myocardial band. If any of these geodesic tracts are to be recognized as subsidiary anatomical entities, they should be revealed by our current technique, which measures the primary direction of diffusion, and hence shows the principal mechanical connection between cells or volumes of cells. Since none of our data reflected such notions, we conclude that presumed toroids of myocytes are just as artifactual as the proposed unique band.

According to conventional wisdom, all myocytes making up the ventricular walls are orientated tangentially so as to exert systolic constrictive forces (Frank, 1901). Subsequent findings showed some deviation from this scheme, with some myocytes oriented relatively transversely, albeit with the transverse orientation not exceeding 10° (Streeter et al., 1969). More recent findings revealed far greater transmural angulation of some of the aggregated myocytes (Lunkenheimer et al., 2006). Our current findings endorse these latter findings, showing spiraling of tracks in the transverse plane at the left ventricular apex (Geerts et al., 2002). Our findings also show that both the helical angle of the aggregated myocytes, and the transmural angulations, reflect the local orientation of a volume of myocytes. This volume is connected to other volumes by means of virtual pathways that spiral through the entirety of the ventricular mass. As indicated, other recent reports have documented substantially greater angles of transmural intrusion than those either found in this study, or in the work of Geerts et al (Lunkenheimer et al., 2006). We speculate that this may well reflect an inherent characteristic in the technique of DTMRI. The chosen voxels of interest measure $\sim 1 \text{ mm}^3$, whilst the average myocyte measures $\sim 20 \times 20 \times 100 \mu\text{m}^3$. The primary eigenvector, therefore, represents the mean direction in the chosen voxel of at least 25,000 myocytes, some of which may diverge at significantly greater angles relative to the tangential plane of the cavities. The technique, therefore, is unable to detect changes of angulation between adjacent myocytes, albeit retaining its validity to detect potential chains of myocytes that have dimensions on the scale of centimeters.

It seems paradoxical that even though this, and other recent studies, show no evidence for the existence of myocardial anatomical structures of higher order than the myocyte itself, there is a remarkable similarity in the pathways shown in separate hearts. Virtual preferential pathways extending from certain points in the myocardium of one heart, therefore, can be predicted with a certain statistical probability in another heart. What are the anatomical substrates producing this conclusion? We hypothesize that the local architecture within the overall three-dimensional myocardial mesh is

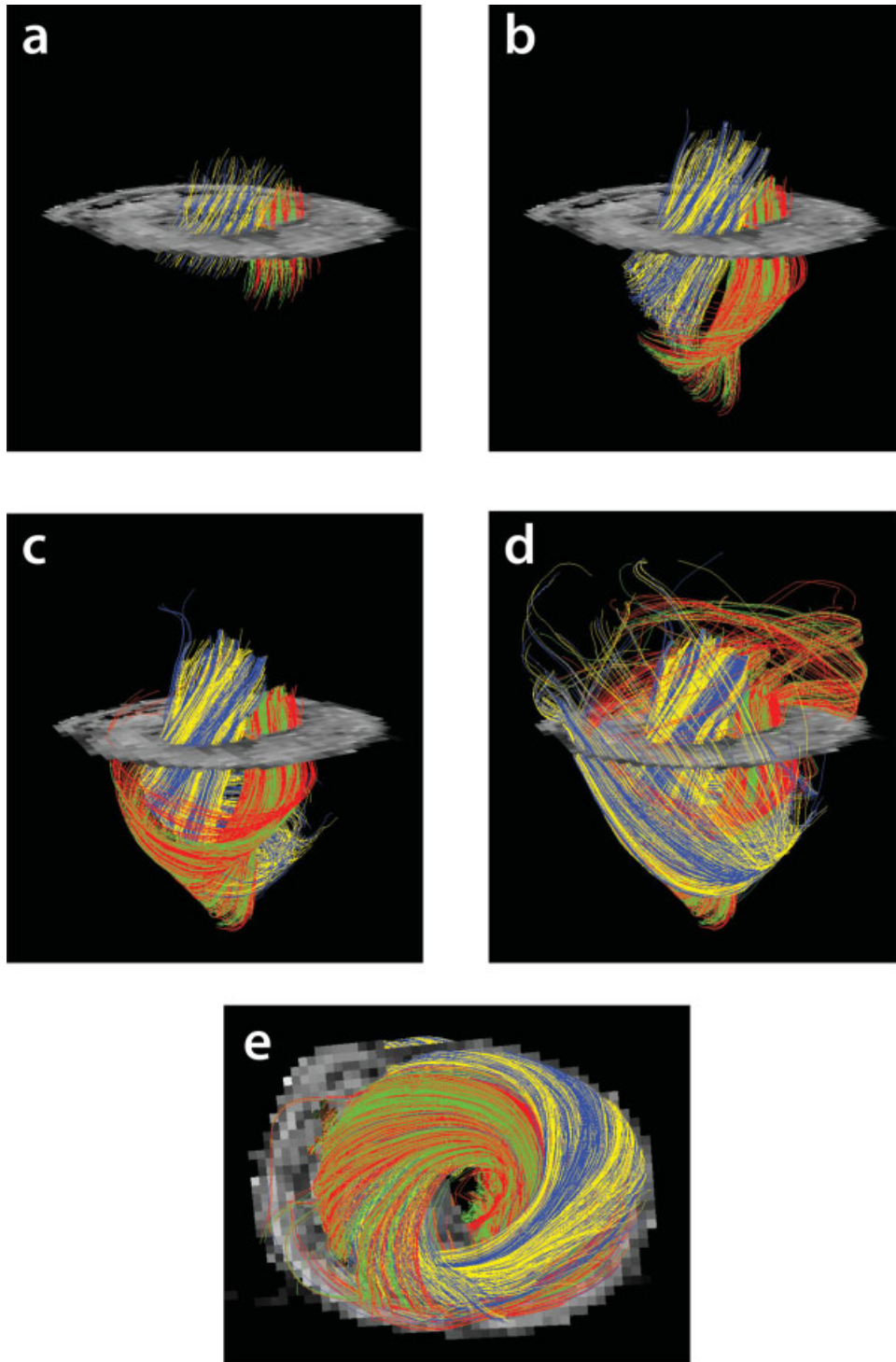


Fig. 6. The papillary muscles. The antero-lateral papillary muscle is represented by alternating blue and yellow colors and the postero-medial papillary muscle is represented by green and red colors. Images (a-d) show that myocytes from the papillary muscles consti-

tute the left ventricular cone. Image e shows the vortex of the left ventricular apex myocytes. The pathways intrude from epicardium to endocardium by means of a right hand helix movement about a transverse circular axis.

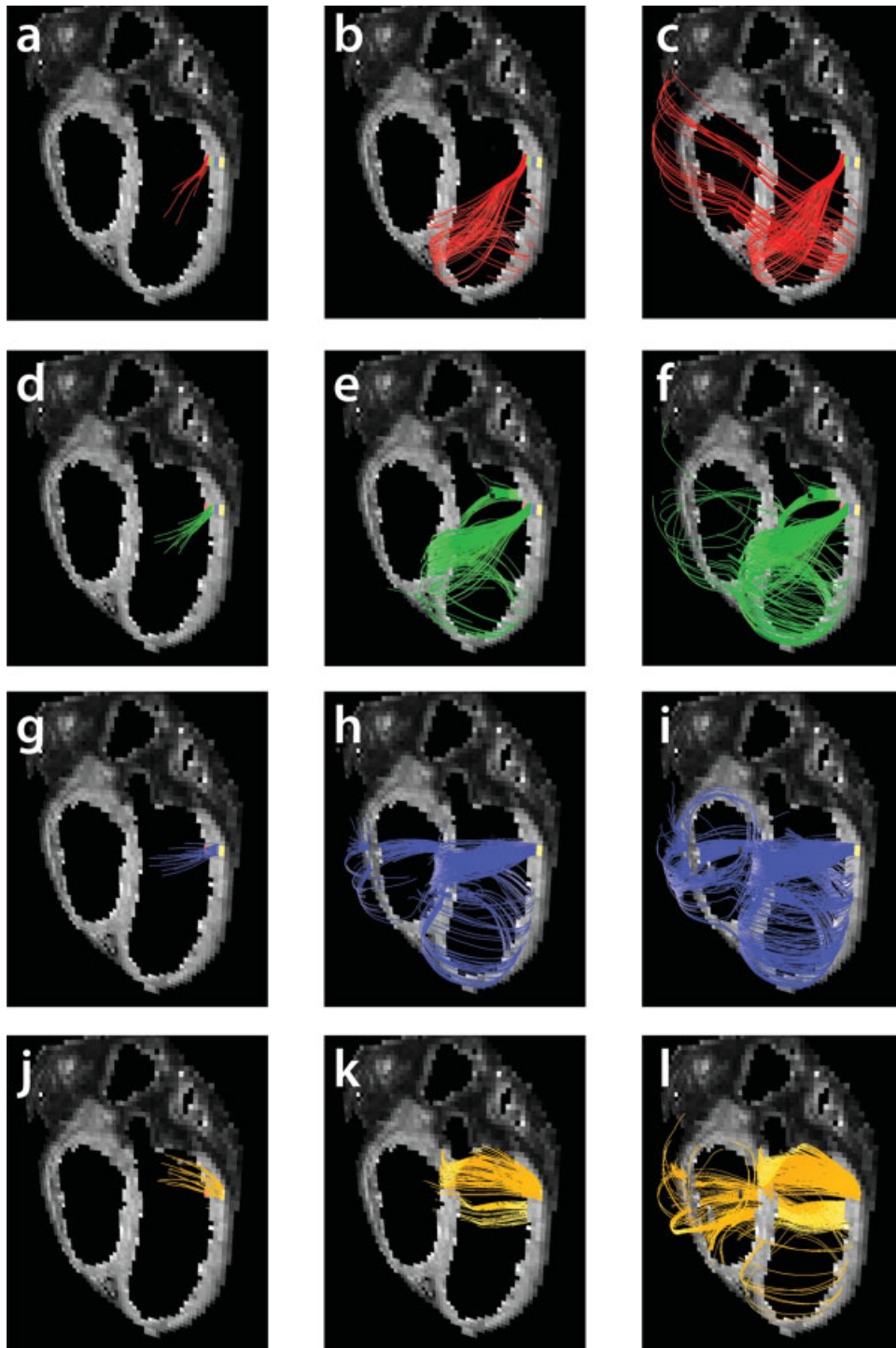


Fig. 7. Track progression from a transmural segment of the left ventricular basal free wall. The wall spans four voxels, the red being endocardial, the green and blue belonging to the midwall and the yellow being epicardial. Also here tracks smoothly change helical and transmural intrusion angles to travel between endocardial, midwall, and epicardial positions.

dependent upon two factors. The first is the orientation in space of the long axis of the myocyte, which is its longitudinal vector. The second is the net vector of the aggregated myocytes, the branches with adjacent myo-

cytes determining the strength of communication in any three-dimensional direction. In addition, when examining the myocardium with a technique such as diffusion tensor imaging, spatial resolution plays an important

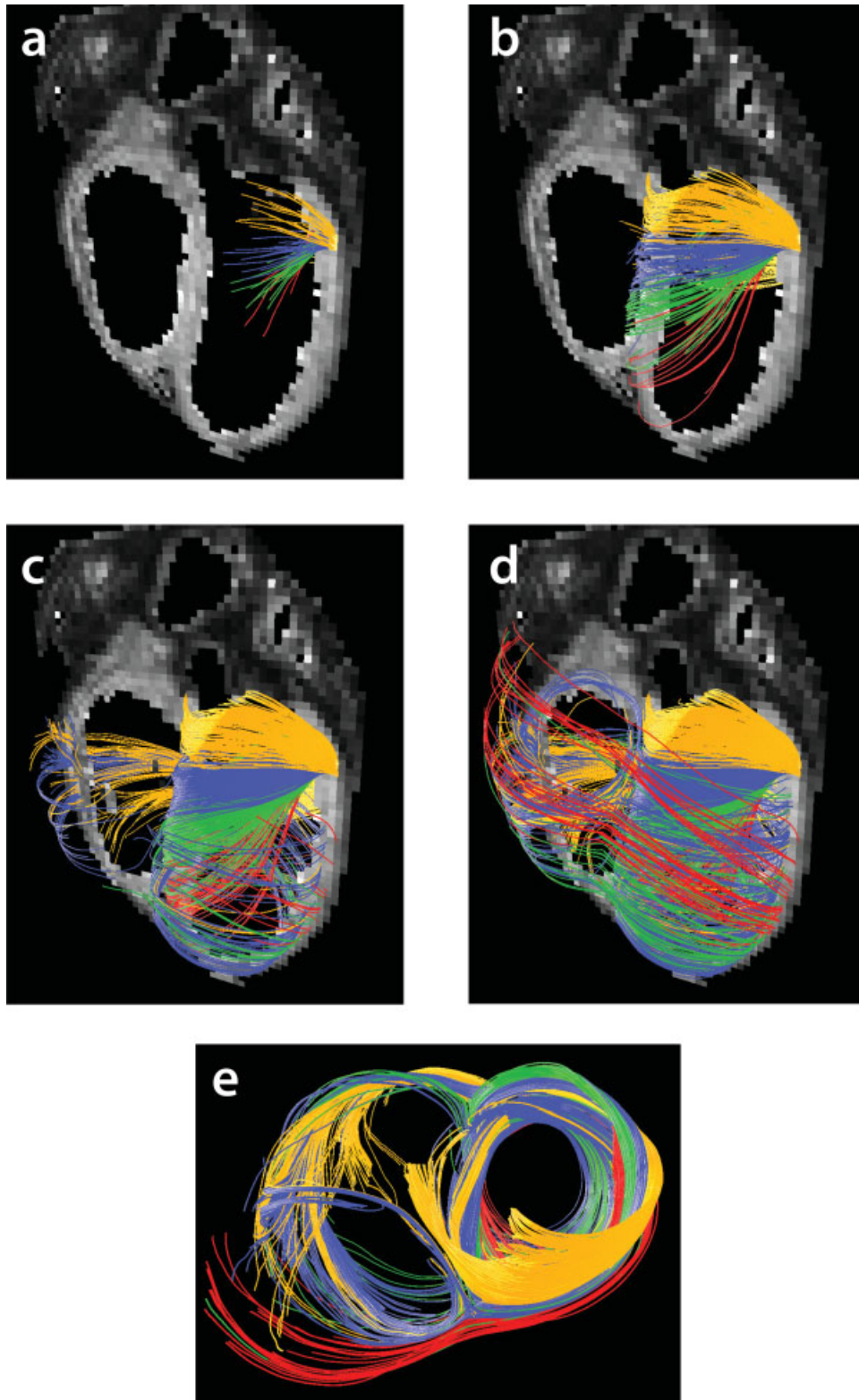


Fig. 8. The same tracks as in Fig. 6 is here shown together in images (a–d). Image (e) shows the basal circumference of the left ventricle. Like in the apex, pathways intrude from epicardium to endocardium by means of a right hand helix movement about a transverse circular axis. The figure shows clearly the right ventricle is composed by tracks from the parietal walls of the left ventricle.

constraining role, since the sum of these factors governs the result obtained from any given voxel of interest.

A significant number of previous studies have either disregarded or underestimated the extent of transmural intrusion of myocytes within the ventricular walls (Frank, 1869; Streeter et al., 1969). As such, mathematical models of left ventricular function have relied upon the construction of the myocardium from “shells” of myocytes, each “shell” containing cells with different angles of inclination relative to the equatorial plane (Hunter and Smith, 1988; Nielsen et al., 1991). The interaction between different layers within the myocardium has, therefore, been thought to be mediated via the connective tissue framework, with special struts presumed to span the ventricular wall from epicardium to endocardium (Ingels, 1997; Caulfield and Janicki, 1997). We do not disregard the potential for the stroma to exert a significant modulating action in terms of diverting forces of myocytic contraction and thickening away from the tangential plane of the ventricles. On the basis of our present findings, nonetheless, we hypothesize that distant transmurally placed myocardial regions are structurally connected along the long axes of the aggregated chains of myocytes so as to enable total contraction in a functionally coordinated manner. According to the brilliantly simple concept of Sallin, the presence of both helical and circular myocytes may alone explain the emptying of the cardiac chambers in the face of physiological myocytic shortening of maximally 15% (Sallin, 1969). Our findings serve to explain the necessary functional interaction between myocytes with different angles of inclination. Notwithstanding the fact that recent studies have proposed that rearrangements of sheets of myocytes are primary determinants of mural thickening (LeGrice et al, 1995; Costa et al., 1999; Harrington et al., 2005), to the best of our knowledge myocytic shortening and thickening are still the fundamental motors of the myocardium. Any purported secondary structure thus serves only as a means of transmitting force. To our knowledge, ours is the first study to show the presence of pathways formed by interconnected myocytes, albeit without any anatomical compartmentation, that extend throughout the ventricular mass in a highly reproducible manner according to varying local helical and transmural angulations. This pattern of preferential pathways is an inherent quality of the three-dimensional myocardial mesh, dependent upon the regional orientation and branching of individual myocytes, and may have significant functional implications.

LITERATURE CITED

- Caulfield JB, Janicki JS. 1997. Structure and function of myocardial fibrillar collagen. *Technol Health Care* 5:95–113.
- Costa KD, Takayama Y, McCulloch AD, Covell JW. 1999. Laminar fiber architecture and three-dimensional systolic mechanics in canine ventricular myocardium. *Am J Physiol* 276:H595–H607.
- Dorri F, Niederer PF, Redmann K, Lunkenheimer PP, Cryer CW, Anderson RH. 2007. An analysis of the spatial arrangement of the myocardial aggregates making up the wall of the left ventricle. *Eur J Cardiothorac Surg* 31:430–437.
- Frank O. 1901. Isometrie und Isotonie des Herzmuskels. *Z Biol* 41:14–34.
- Geerts L, Bovendeerd P, Nicolay K, Arts T. 2002. Characterization of the normal cardiac myofiber field in goat measured with MR-diffusion tensor imaging. *Am J Physiol Heart Circ Physiol* 283:H139–H145.
- Grant R. 1965. Notes on the muscular architecture of the left ventricle. *Circulation* 32:301–308.
- Harrington KB, Rodriguez F, Cheng A, Langer F, Ashikaga H, Daughters GT, Criscione JC, Ingels NB, Miller DC. 2005. Direct measurement of transmural laminar architecture in the anterolateral wall of the ovine left ventricle: new implications for wall thickening mechanics. *Am J Physiol Heart Circ Physiol* 288:H1324–H1330.
- Holmes AA, Scollan DF, Winslow RL. 2000. Direct histological validation of diffusion tensor MRI in formaldehyde-fixed myocardium. *Magn Reson Med* 44:157–161.
- Hsu EW, Muzikant AL, Matulevicius SA, Penland RC, Henriquez CS. 1998. Magnetic resonance myocardial fiber-orientation mapping with direct histological correlation. *Am J Physiol* 274:H1627–H1634.
- Hunter PJ, Smaill BH. 1988. The analysis of cardiac function: a continuum approach. *Prog Biophys Mol Biol* 52:101–164.
- Ingels NB, Jr. 1997. Myocardial fiber architecture and left ventricular function. *Technol Health Care* 5:45–52.
- Jouk PS, Usson Y, Michalowicz G, Grossi L. 2000. Three-dimensional cartography of the pattern of the myofibres in the second trimester fetal human heart. *Anat Embryol (Berl)* 202:103–118.
- Krehl L. 1891. Beiträge zur Kenntniss der Füllung und Entleerung des Herzens. *Abh Math Phys Kl Saechs Akad Wiss* 17:341–362.
- LeGrice IJ, Smaill BH, Chai LZ, Edgar SG, Gavin JB, Hunter PJ. 1995. Laminar structure of the heart: ventricular myocyte arrangement and connective tissue architecture in the dog. *Am J Physiol* 269:H571–H582.
- Lev M, Simkins C. 1956. Architecture of the human ventricular myocardium; technic for study using a modification of the Mall-MacCallum method. *Lab Invest* 5:396–409.
- Lunkenheimer PP, Redmann K, Kling N, Jiang X, Rothaus K, Cryer CW, Wubbeling F, Niederer P, Heitz PU, Ho SY, Anderson RH. 2006. Three-dimensional architecture of the left ventricular myocardium. *Anat Rec A Discov Mol Cell Evol Biol* 288:565–578.
- Mall FP. 1911. On the muscular architecture of the ventricles of the human heart. *Am J Anat* 11:211–278.
- Nielsen PM, Le GI, Smaill BH, Hunter PJ. 1991. Mathematical model of geometry and fibrous structure of the heart. *Am J Physiol* 260:H1365–H1378.
- Parker GJ, Haroon HA, Wheeler-Kingshott CA. 2003. A framework for a streamline-based probabilistic index of connectivity (PICO) using a structural interpretation of MRI diffusion measurements. *J Magn Reson Imaging* 18:242–254.
- Pettigrew JB. 1864. On the arrangement of the muscular fibres in the ventricles of the vertebrate, with physiological remarks. *Philos Trans* 154:445–500.
- Press W, Teukolsky S, Flannery B. 2007. *Numerical Recipes. The art of scientific computing*. 3rd ed. Cambridge: Cambridge University Press.
- Sallin EA. 1969. Fiber orientation and ejection fraction in the human left ventricle. *Biophys J* 9:954–964.
- Streeter DD, Jr, Spotnitz HM, Patel DP, Ross J, Jr., Sonnenblick EH. 1969. Fiber orientation in the canine left ventricle during diastole and systole. *Circ Res* 24:339–347.
- Torrent-Guasp F, Kocica MK, Corno AF, Komeda M, Carreras-Costa F, Flotats A, Cosin-Aguillar J, Wen H. 2005. Towards new understanding of the heart structure and function. *Eur J Cardiothorac Surg* 27:191–201.
- Torrent-Guasp F, Ballester M, Buckberg GD, Carreras F, Flotats A, Carrio I, Ferreira A, Samuels LE, Narula J. 2001. Spatial orientation of the ventricular muscle band: physiologic contribution and surgical implications. *J Thorac Cardiovasc Surg* 122:389–392.
- Wu EX, Wu Y, Tang H, Wang J, Yang J, Ng MC, Yang ES, Chan CW, Zhu S, Lau CP, Tse HF. 2007. Study of myocardial fiber pathway using magnetic resonance diffusion tensor imaging. *Magn Reson Imaging* 25:1048–1057.